GREAT scholarship. We also thank Moli Energy (1990), Limited, for financial support of this work.

Manuscript received April 30, 1996.

Simon Fraser University assisted in meeting the publication costs of this article.

REFERENCES

1. B. E. Warren, *Phys. Rev.*, **9**, 693 (1941).
2. R. E. Franklin, *Proc. R. Soc. London, Ser. A*, **209**, 196 (1951).
3. Y. Liu, J. S. Xue, T. Zheng, and J. R. Dahn, *Carbon*, **34**, 193 (1996).
4. M. Kalliat, C. Y. Kwak, and P. W. Schmidt, in *New Approaches in Coal Chemistry*, B. D. Blaustein, B. C. Bockrath, and S. Friedman, Editors, p. 3, American Chemical Society, Washington, DC (1981).
5. T. Zheng, Y. Liu, E. W. Fuller, S. Tseng, U. von Sacken, and J. R. Dahn, *This Journal*, **142**, 2581 (1995).
6. T. Zheng, J. S. Xue, and J. R. Dahn, *Chem. Mater.*, **8**, 383 (1996).
7. N. Sonobe, M. Ishikawa, and T. Iwasaki, Paper 2B10 presented at the 35th Battery Meeting in Japan, Nagoya, Japan, Nov. 14-16, 1994, Extended Abstracts p. 49.
8. J. S. Xue and J. R. Dahn, *This Journal*, **142**, 3668 (1995).
9. W. Xing, J. S. Xue, and J. R. Dahn, *This Journal*, **143**, 3046 (1996).
10. T. Zheng, Q. Zhong, and J. R. Dahn, *ibid.*, **142**, L211 (1995).
11. A. Guinier and G. Fournet, *Small Angle Scattering of X-Rays*, John Wiley & Sons, Inc., New York (1955).
12. A. Gibaud, J. S. Xue, and J. R. Dahn, *Carbon*, **34**, 499 (1996).

A Hydrogen-Nitric Oxide Cell for the Synthesis of Hydroxylamine

Kiyoshi Otsuka,* Hidenori Sawada, and Ichiro Yamanaka

Department of Chemical Engineering, Tokyo Institute of Technology, Ookayama, Meguro-ku, Tokyo 152, Japan

ABSTRACT

A H_2-NO fuel cell was designed for the synthesis of hydroxylamine in the gas phase. The hydroxylamine produced was trapped in an aqueous solution of H_2SO_4 held in a silica-wool disk used as an electrolyte barrier for H_2 and NO. Among the cathode electrocatalysts tested, iron-phthalocyanine (Fe-Pc) impregnated in graphite was the most favorable one for selective synthesis of hydroxylamine. Active carbon and carbon whiskers used to support the Fe-Pc enhanced the formation of hydroxylamine remarkably. The carbon itself slightly catalyzed the formation of N_2O and NH_3. Excluding the effects of the support, Fe-Pc catalyzed the electrochemical synthesis of hydroxylamine with high selectivity (≈100%). Applied voltage across the cell did not appreciably enhance the formation of hydroxylamine. The reaction under short-circuit conditions was most favorable for the synthesis of hydroxylamine. It is suggested that the reduction of NO occurs on the Fe^{2+} site of Fe-Pc with protons and electrons transferred from the anode. The very selective synthesis of hydroxylamine over Fe-Pc must be ascribed to an Fe^{2+} site isolated by phthalocyanine ring. This isolation prohibits both the formation of N_2O through the intramolecular elimination of H_2O from the adjacent NHO intermediates and the formation of N_2 and NH_3 through the breaking of N–O bonds.

Salts of hydroxylamine and their solutions are of great industrial importance as intermediates, particularly in the production of caprolactam, the monomer for nylon 6. Industrial production of hydroxylamine is carried out by catalytic hydrogenation of nitric oxide or nitric acid. Usually, the product is an aqueous solution of a salt $NH_2OH \cdot HA$ (where HA is an acid such as sulfuric or phosphoric acid) or (NH_3OH) A, rather than free hydroxylamine.

Catalytic hydrogenation of nitric oxide is usually performed by the contact of hydrogen and a substrate with a suitable catalyst such as platinum. An electrochemical hydrogenation technique using the hydrogen supplied electrochemically through a proton-conducting membrane was first demonstrated by Langer and co-workers.[1,2] In this method, hydrogen flows in one side of an electrolyte barrier while nitric oxide passes in the other side. The electrolyte phase is sandwiched by porous, catalytic electrodes. Under operating conditions, hydrogen is dissociated at one electrode, being transformed into protons and electrons. The protons are conducted through the electrolyte, while electrons are transferred through the external circuit. Hydrogenation of nitric oxide occurs on the counter catalytic electrode with a transfer of protons and electrons. Some of the protons conducted to the cathode may be discharged as evolving hydrogen molecules into the gas phase. The cell voltage and the rate of hydrogen supplied to the cathode can be controlled by an external resistive circuit or a variable applied potential.

* Electrochemical Society Active Member.

The overall reactions described above may be represented as

Anode

$$H_2 \rightarrow 2H^+ + 2\,e^- \quad E^\circ = 0\ V \qquad [1]$$

Cathode

$$2NO + 2H^+ + 2e^- \rightarrow N_2O + H_2O \quad E^\circ = 1.59\ V \qquad [2]$$

$$2NO + 4H^+ + 4e^- \rightarrow N_2 + H_2O \quad E^\circ = 1.68\ V \qquad [3]$$

$$NO + 3H^+ + 3e^- \rightarrow NH_2OH \quad E^\circ = 0.38\ V \qquad [4]$$

$$NO + 5H^+ + 5e^- \rightarrow NH_3 + H_2O \quad E^\circ = 0.73\ V \qquad [5]$$

$$2H^+ + 2e^- \rightarrow H_2 \quad E^\circ = 0\ V \qquad [6]$$

where the standard redox potentials [*vs.* normal hydroen electrode (NHE)] for each reaction are also indicated.

We can expect that hydrogenation of NO would take place without applying a potential across the cell. In other words, the system may work under short-circuit conditions. When we put a load in the outer circuit, the system generates electricity as well as useful chemicals, in this case NH_2OH. The advantages of this concept have already been discussed by many researchers.[1-4] However, the selective synthesis of NH_2OH by this technique has not been successful because of a lack of suitable catalysts. The chemical properties of NO, HNO_2, and NO_2, and their electrochemical reduction on Pt electrodes, have been reviewed by Snider and Johnson.[5] There have been a number of studies on the electrochemical reduction of NO on a variety of electrodes.[5-8]

However, the selectivity and current efficiency for hydroxylamine formation have not been satisfactory.

Therefore, the first purpose of this work is to explore an active and selective electrocatalyst for the synthesis of NH_2OH using a H_2-NO cell reactor in the gas phase under mild reaction conditions. Second, the catalytic behavior of the best cathode and reaction mechanism of NH_2OH formation are described in detail.

Experimental

The NO-H_2 cell reactor used and the principle of the experimental procedure are shown schematically in Fig. 1a. The reactor was connected to a conventional gas flow system. For the measurement of the anode and cathode potentials, a potentiostat-galvanostat (Hokuto HA-301, HB-104) and a standard Ag/AgCl electrode (0.196 V *vs.* NHE) were used with a KCl salt bridge connected to a H_2SO_4-membrane as demonstrated in Fig. 1b. The anode was prepared from a physical mixture of Pt black (20 mg), graphite (50 mg), and Teflon powder (7 mg). The mixture was pressed and shaped into a wafer (20 mm diam) on a hot plate at 393 K. The cathode electrocatalysts tested in this work were metal phthalocyanines, iron tetraphenyl porphyrin, $FeSO_4$, Pt, Ru, and Pd. For the preparation of the cathode, the catalytic components examined were first dissolved into dichloromethane or water. In the cases of noble metals, the corresponding chlorides were the starting compounds. After the solvents were dried out at *ca.* 373 K, the graphite (60 mg) impregnated with the catalytic components was thoroughly mixed with Teflon powder (7 mg) before being hot-pressed into a wafer (20 mm diam). For the preparation of the noble metal-added cathodes, the graphites impregnated with H_2PtCl_6, $PdCl_2$, and $RuCl_3$ were reduced at 573 K in a flow of hydrogen for 2 h. The content of the catalytic components was adjusted to be 0.075 mole percent (m/o) against the mole of carbon of the host graphite. The proton-conducting separator was an aqueous solution of H_2SO_4 (5.0 *M*, 0.7 g) held in a silica-wool disk (26 mm diam, 2 mm thickness) unless otherwise stated. The superficial surface area of both electrodes was 3.1 cm^2.

NO was carried with helium into the cathode compartment. Hydrogen and water vapor (added to prevent the electrolyte from drying) were passed through the anode compartment. The total gas pressure for both cathode and anode sides was 101 kPa. The reaction was performed under the following standard reaction conditions unless otherwise described: short-circuit; temperature = 300 K; reaction time = 2 h; [cathode conditions] $p(NO)$ = 9 kPa, $p(He)$ = 92 kPa, flow rate = 10 ml (STP) min^{-1}; [anode conditions] $p(H_2)$ = 91 kPa, $p(H_2O)$ = 4 kPa, $p(He)$ = 6 kPa, flow rate = 20 ml (STP) min^{-1}.

The products in the gas phase (N_2 and N_2O) were analyzed by on-line gas-chromatography. All the hydroxylamine and ammonia produced were dissolved in the electrolyte (H_2SO_4, H_3PO_4, or $HClO_4$) held in a silica wool separator. These two products were extracted with distilled water before being subjected to the following analyses.

The quantitative analysis of hydroxylamine was performed according to the method by Pesselman *et al.*[9] Hydroxylamine reacts readily with acetone to form acetone oxime in acidic solutions. Thus, the hydroxylamine extracted from the silica-wool disk was reacted with acetone at 323 K for 40 min. The acetone oxime produced was extracted with diethyl ether. The extracted solution was analyzed by gas chromatography using a PEG-20 M capillary column. The quantitative analysis of ammonia formation was performed with a modified Nessler test.[10]

Special care was taken to calibrate absorbance at 400 nm *vs.* standard solutions of ammonia because the calibration curves depend on the amount of the hydroxylamine existing in the standard solutions. The calibration for NH_3 concentration was performed at ten different NH_2OH/NH_3 ratios.

All the reagents used in this work were extra pure grade purchased from Wako Pure Chemical Company and Kanto Chemical Industry. Phthalocyanines and Fe-tetraphenylporphyrin were supplied from Japan Energy Company. Graphite (Wako), carbon whisker (Asahi Chemical Industry), active carbon (supplied from Boreskov Institute of Catalysis), and carbon black (Japan Energy Company) used as the cathode were treated in HCl aq. (6 *M*) and thoroughly washed with distilled water.

All experiments were performed using fresh electrodes and silica-wool disks with fresh electrolyte because the extraction of hydroxylamine and ammonia from the electrode and silica-wool disk caused their fracture. The reproducibility in the preparation of a set of electrode-electrolyte systems was checked on the basis of the amounts of each product under the same experimental conditions. A carefully prepared cell system showed reproducibility of approximately ±10%.

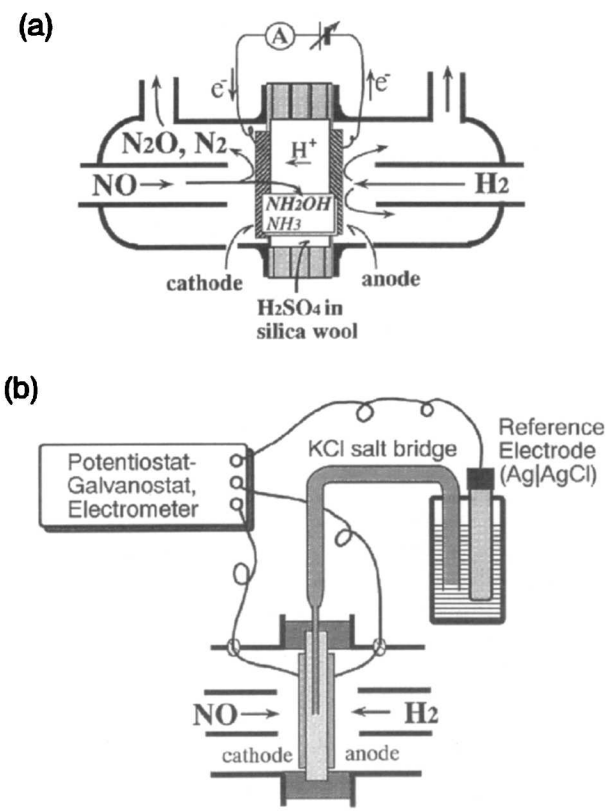

Fig. 1. Schematic diagrams of the NO-H_2 cell reactor (a) and the method of the measurement of cathode and anode potentials (b) during the reaction.

Results and Discussion

Comparison of electrocatalytic activities of the additives in the graphite cathode.—Favorable electrocatalysts for the synthesis of hydroxylamine have been examined under standard reaction conditions. The results are shown in Table I. For all the catalysts in Table I, no N_2 or only a trace was observed. Compared to the results of the graphite cathode without additives, the catalytic functions of $FeSO_4$, Fe-phthalocyanine (Fe-Pc), Pt, Ru, and Pd are listed in Table I. Among the electrocatalysts in Table I, Pt is the most active catalyst for reduction of NO into NH_2OH, NH_3, and N_2O. However, the selectivity to NH_2OH for this catalyst is not very high (≈63%). This low selectivity toward NH_2OH formation is also true for the catalytic performance of Ru. With regard to the selectivity to hydroxylamine, the result for Fe-Pc/Gr is most favorable (90%). The catalytic activity of the Fe-Pc for the hydroxylamine formation is the third highest among the additives in Table I. Thus, we have chosen this material as one of the most prospective electrocatalysts for selective synthesis of hydroxylamine.

Table I. Electrocatalytic reactivity for the reduction of NO over various cathdes.

Cathode	Charge Passed (C)	Products (μmol) N_2O	NH_3	NH_2OH	Selectivity to NH_2OH (%)
Graphite only	8.4	6.5	11	6.4	21
$FeSO_4$/Gr	18.0	37	19	7.9	7.8
Fe-Pc/Gr	84.0	7.4	13	255	90
Fe-TPP/Gr	6.4	3.4	8.7	4.4	22
Co-Pc/Gr	6.3	3.9	7.6	5.8	28
Cu-Pc/Gr	< 2	0	0	0	—
Pt/Gr	232.0	58	152	448	63
Ru/Gr	153.0	18	134	291	63
Pd/Gr	86.0	237	0	125	20

Standard reaction conditions: T = 300 K; concentration of H_2SO_4 = 5 M; content of additive = 0.075 m/o; reaction time = 2 h. Cathode: $p(NO)$ = 9 kPa, $p(He)$ = 92 kPa, F = 10 $cm^3\ min^{-1}$. Anode: $p(H_2)$ = 91 kPa, $p(H_2O)$ = 4 kPa, $p(He)$ = 6 kPa, F = 20 $cm^3\ min^{-1}$.

Effect of carbon materials as the support of Fe-Pc.—Active carbon (AC), carbon whisker (CW), and carbon black (CB) were tested as the cathode carbon materials instead of graphite (Gr). The results obtained for these carbon materials added with Fe-phthalocyanine (0.075 m/o) under standard experimental conditions are summarized in Table II. AC and CW enhanced the formation of hydroxylamine remarkably. The average current per superficial surface area for the Fe-Pc/CW was 11 mA cm^{-2}. The selectivity to hydroxylamine was also improved for these carbon materials. Among the cathodes examined, the Fe-Pc/AC showed a remarkably high selectivity to hydroxylamine (~99%). The favorable effects of AC and CW, especially upon the rate of reaction, might be ascribed to the dispersion of catalyst (Fe-Pc) on the carbon with high surface area. The specific surface areas measured for the carbon materials were as follows; Gr(<0.1)<CW(22)<CB(110)<AC(287 $m^2\ g^{-1}$). The porosities or the pore volume of the carbon materials were Gr(<0.01) < CW(0.029) < AC(0.584) < CB(1.009 $cm^3\ g^{-1}$). These orders suggest that the activities of the cathodes in Table II cannot be explained in terms of only the dispersion of the catalysts or the porosity of the carbons.

In order to study the roles of carbons and Fe-Pc in the electrocatalytic formation of hydroxylamine and to propose the reaction mechanism, we have concentrated our efforts on the catalytic reactions over the Fe-Pc/Gr cathode because this is the most stable electrode among those in Table II.

Effects of different electrolytes on the reduction of NO.—The hydroxylamine and ammonia produced accumulate in the electrolyte (H_2SO_4) in a silica-wool disk as their sulfates. Therefore, it is expected that the formation of hydroxylamine and ammonia will depend on the kinds of electrolytes. Table III demonstrates the results of NO reduction using different electrolytes. The experiments were performed under standard conditions except for changing the electrolyte in a silica wool disk. When acidic electrolytes (H_3PO_4, H_2SO_4, and $HClO_4$) were used, hydroxylamine was produced with fairly good selectivity. However, hydroxylamine was not formed at all and N_2O was the main product in the case of 2 M KOH as an electrolyte. Although 5 M $HClO_4$ enhanced the formation of hydroxylamine compared to 5 M H_2SO_4, an aqueous H_2SO_4 electrolyte was used for further studies since a better selectivity to hydroxylamine as well as a better reproducibility were guaranteed for the reactions using this electrolyte.

Table III. Effect of different electrolytes in the membrane on the reduction of NO.

Electrolyte	Charge passed (C)	Products (μmol) N_2	N_2O	NH_3	NH_2OH	Selectivity to NH_2OH (%)
5 M H_3PO_4	80	0	20	22	201	76
5 M H_2SO_4	84	0	7.4	13	255	90
5 M $HClO_4$	140	0	3.0	64	376	85
2 M KOH	32	3.6	122	9	0	0

Under standard reaction conditions.

Optimum concentration of H_2SO_4.—The rate of hydroxylamine formation depended considerably on the concentration of the H_2SO_4 electrolyte. The rate was at a maximum at a concentration 3 M H_2SO_4 as indicated in Fig. 2. The current (or the charge passed) and the rates of formation of products decreased at concentrations of H_2SO_4 > 3 M. However, the selectivity to hydroxylamine remained high (~88%) at greater than 3 M H_2SO_4. The total current efficiency calculated from the amount of each product assuming the cathode reactions were those given in Eq. 2, 4, and 5 was always 100% within an experimental error of ±5%.

Effect of Fe-Pc content in the cathode.—The content of Fe-Pc in graphite under standard conditions was 0.075 m/o with respect to the carbon content. As can be seen in Fig. 3, the amount of hydroxylamine formed increased linearly with the content of Fe-Pc at up to 0.15 m/o. The selectivity to hydroxylamine was higher than 90% at the content of Fe-Pc greater than 0.075 m/o. However, excess addition of Fe-Pc beyond 0.15 m/o decreased the formation of hydroxylamine due to a poor contact of Fe-Pc with graphite and electrolyte.

Kinetic studies on the synthesis of hydroxylamine.—In order to get information about the catalytic functions of Fe-Pc and the reaction mechanism for the synthesis of hydroxylamine, the effects of various kinetic parameters on the reaction have been examined.

Kinetic curves.—Figure 4 shows the kinetic curves of each product and the charge passed as a function of reaction time. The experiments were performed under standard conditions. The amounts of each product and the charge passed increase proportionally to the reaction time irrespective of the accumulation of hydroxylamine and ammonia in the electrolyte. The hydroxylamine and ammonia formed at the cathode must instantly react with H_2SO_4 to be converted into $(NH_3OH)_2SO_4$ and $(NH_4)_2SO_4$, respectively. The consumption of H_2SO_4 in the silica-wool disk was less than 20% after 3 h reaction under the experimental conditions in Fig. 4. The results in Fig. 4 indicate that such consumption of H_2SO_4 would not severely reduce the rate of reaction.

Effect of the partial pressures of NO and H_2.—The effect of the partial pressure of NO on the rate of formation of each product was measured under standard reaction condi-

Table II. Effect of carbon material as the support of Fe-phthalocyanine on the synthesis of hydroxylamine.

Cathode	Charge passed (C)	Products (μmol) N_2O	NH_3	NH_2OH	Selectivity to NH_2OH(%)	Conversion of NO (%)
Fe-Pc/Gr	84	7.4	13	255	90	6.4
Fe-Pc/Ac	207	2.6	0	661	99	15.2
Fe-Pc/CW	244	2.9	51	718	93	17.6
Fe-Pc/CB	38	9.2	16	88	72	2.8

Under standard reaction conditions.

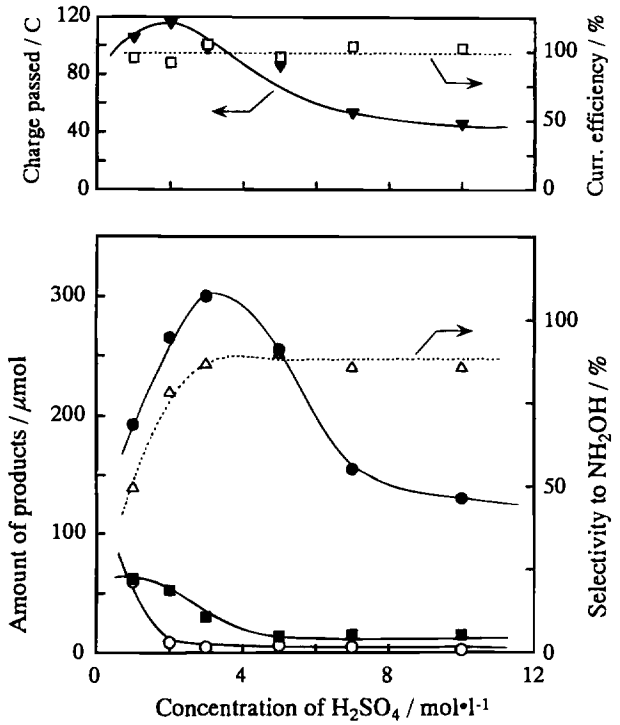

Fig. 2. Effects of the concentration of the electrolyte (H_2SO_4 aq.) on the electrochemical synthesis of hydroxylamine. Under standard reaction conditions. Amount of products: NH_2OH (●), NH_3 (■), N_2O (○). Current efficiency for the sum of products (□), charge passed (▼)

tions. The results are plotted in Fig. 5. The charge passed and the amounts of hydroxylamine and ammonia formed in 2 h increased linearly with the pressure of NO up to 25 kPa and reached a plateau above this pressure. The formation of N_2O was accelerated at above 20 kPa, thus the selectivity to hydroxylamine decreased slightly.

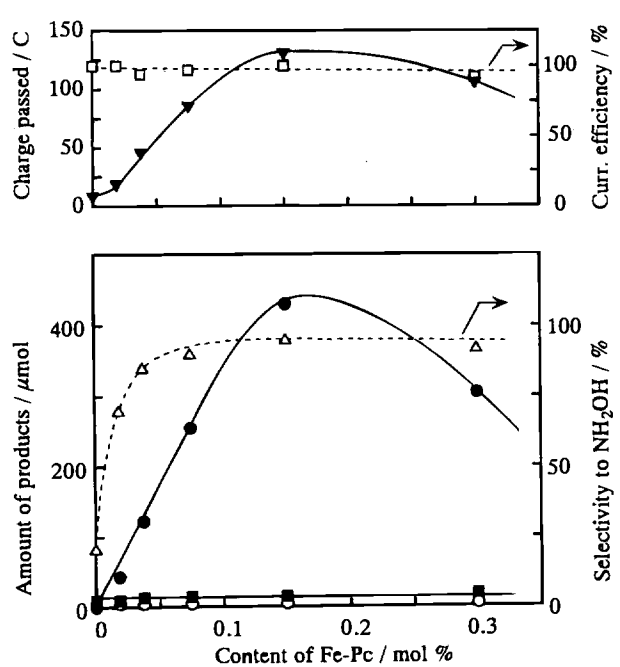

Fig. 3. Effect of the content of Fe-Pc on the electrochemical synthesis of hydroxylamine. Under standard reaction conditions. Amount of products: NH_2OH (●), NH_3 (■), N_2O(○). Current efficiency for the sum of products (□), charge passed (▼)

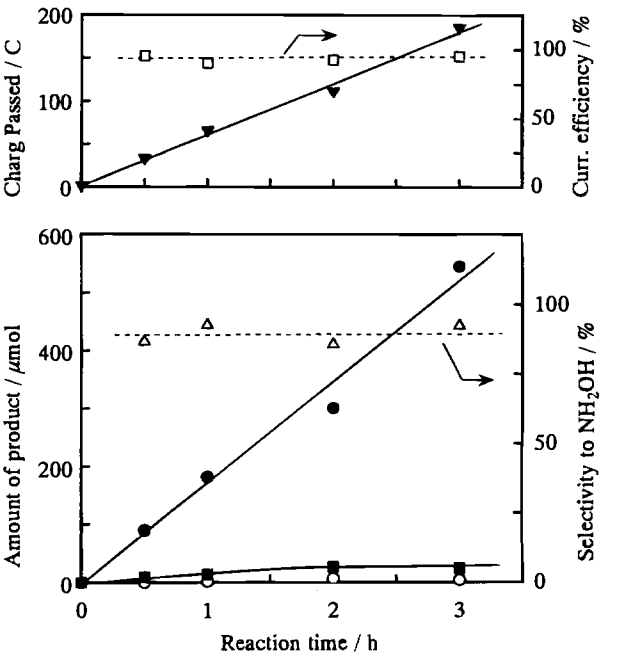

Fig. 4. Reaction profiles with time. Under standard reaction conditions. Amount of products: NH_2OH (●), NH_3 (■), N_2O (○). Current efficiency for the sum of products (□), charge passed (▼).

The partial pressure of hydrogen in the anode compartment affected neither the charge passed nor the rates of formation of each product at the cathode in the hydrogen pressure range of 5-95 kPa.

The kinetic results described above suggest that the oxidation of hydrogen at the anode is fast, and the rate-determining step for the reduction of NO is in the cathode reactions. This was supported by the anode and cathode potentials measured under the same experimental conditions as described below.

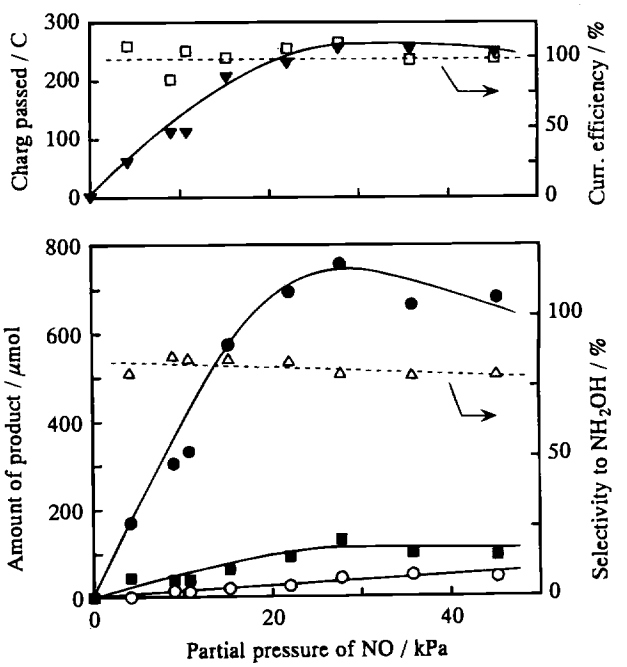

Fig. 5. Effect of the partial pressure of nitric oxide on the formation of products. Under standard reaction conditions. Amount of products: NH_2OH (●), NH_3 (■), N_2O (○). Current efficiency for the sum of products (□), charge passed (▼).

Under open-circuit conditions with the same gas flows as those of standard conditions in the cathode and the anode compartments, the cathode and the anode potentials were 0.83 and −0.13 V (*vs.* Ag/AgCl), respectively. The reduction of NO was started by shorting the circuit. The anode and the cathode potentials were changed to −0.11 V (*vs.* Ag/AgCl) under the short-circuit conditions. Both potentials were the same after correcting the ohmic drops of the lead wires between both electrodes. When the circuit was opened after the reduction of NO for 2 h under short-circuit conditions, the anode potential returned to the original value, *i.e.*, −0.13 V (*vs.* Ag/AgCl). The cathode potential increased rapidly to 0.69 V (*vs.* Ag/AgCl), but never recovered to the original value (0.83 V). This decrease in the open-circuit cathode potential might be ascribed to the accumulation of products. The results described above indicate the existence of a large overpotential at the cathode and a slight one at the anode. These observations strongly support the idea that the rate-controlling step is in the cathode reactions.

Dependence of hydroxylamine formation on the terminal voltage.—The experiments were performed under short-circuit conditions. It is interesting to determine if the hydroxylamine formation is accelerated when a negative potential is applied at the cathode. On the other hand, how does the application of a load in the outer circuit improve the selectivity to hydroxylamine. The results obtained under different terminal voltages (the potential difference between the cathode and the anode) are shown in Fig. 6. Here, zero terminal voltage means short-circuit conditions.

The application of a small negative potential to the cathode with reference to the anode (terminal voltage < 0) increased the charge passed and the amount of hydroxylamine formed in 2 h. However, further application of the negative potential (terminal voltage <−0.05 V) did not enhance either the current or the formation of hydroxylamine. This observation shows that the input of electrical energy is not so effective for enhancing the formation of hydroxylamine.

On the other hand, the application of a load in the outer circuit, increasing the terminal voltage in the positive direction, decreased the current as well as the formation of hydroxylamine. The selectivity to hydroxylamine was not affected appreciably. For the purpose of synthesizing hydroxylamine preferentially, the results in Fig. 6 suggest that the reaction should be performed under short-circuit conditions.

The cathodic and anodic potentials at the terminal voltage covering those of Fig. 6 were measured separately by the method demonstrated in Fig. 1b. Both potentials obtained *vs.* Ag/AgCl are plotted in Fig. 7. The current observed during these experiments and the calculated power output from the outer circuit are also shown in the upper part of Fig. 7. As can be seen in Fig. 7, the anode potential (−0.13 V *vs.* Ag/AgCl) did not change with the terminal voltage when the latter was greater than 0.2 V. The anode potential increased slightly to −0.11 V (*vs.* Ag/AgCl) when the terminal voltage was lowered to −0.20 V due to a small ohmic polarization at the cathode. On the other hand, the cathode potential decreased linearly to the terminal voltage of the cell. Therefore, it should be noted that the sweep of the terminal voltage from +0.2 to −0.2 V on the abscissa of Fig. 6 means the linear decrease in the cathode potential (neglecting a small change in the anode potential described above) from +0.1 V to −0.29 V *vs.* Ag/AgCl.

It should be recalled that the theoretical potentials for the reduction of NO into N_2O, N_2, NH_3, and NH_2OH are 1.39, 1.48, 0.53, and 0.18 V *vs.* Ag/AgCl, respectively. The results in Fig. 7 show that the reduction of NO does not occur at cathode potentials higher than 0.08 V *vs.* Ag/AgCl. Only a small current flows at cathode potentials between 0.40 and 0.08 V. The current increases sharply at the cathode potential <0.08 V *vs.* Ag/AgCl or at the terminal voltage of the cell lower than 0.16 V. Comparison of the results between Fig. 6 and 7 clearly indicates that this current is caused by the reduction of NO to hydroxylamine. The fuel cell power output indicated in Fig. 7 shows the maximum at an operating terminal voltage of ca. 0.10 V. According to the results in Fig. 6, the hydroxylamine formation at this terminal voltage decreased only 30% compared to the short-circuit conditions (terminal voltage = 0 V). Under

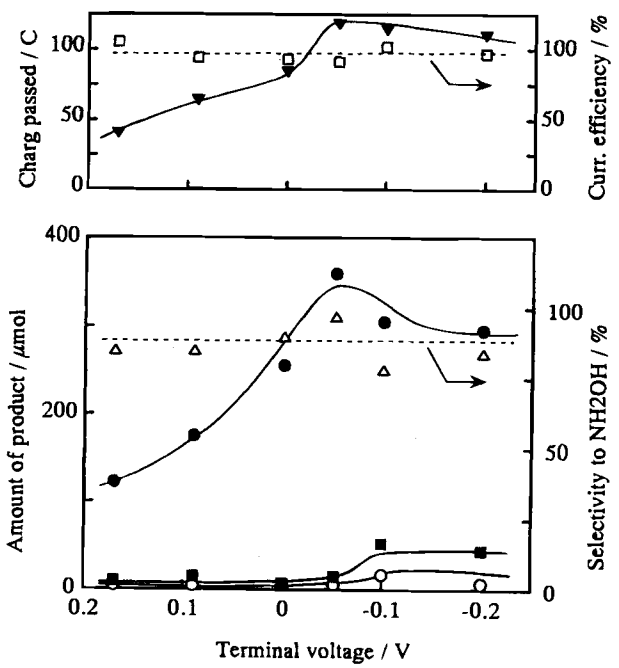

Fig. 6. Reduction of NO as functions of the terminal voltage of the cell. Zero: short-circuit, positive voltage: with a load in the outer circuit, negative voltage: with an applied voltage. Amount of products: NH_2OH (●), NH_3 (■), N_2O (○). Current efficiency for the sum of products (□), charge passed (▼).

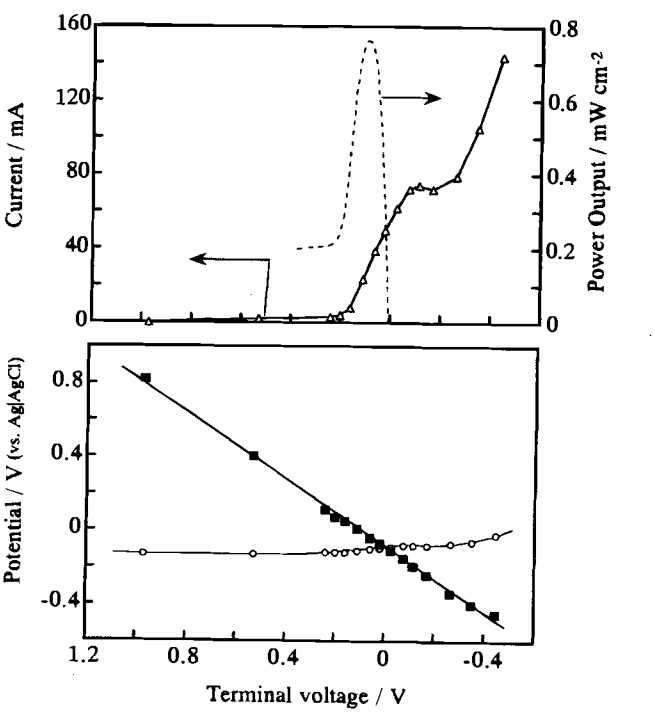

Fig. 7. The anode and cathode potentials, the current and the fuel cell power output as functions of the terminal voltage of the cell. Under standard conditions except for changing the terminal voltage. Cathode potential (■), anode potential (○), current (△), power output (···).

these operating conditions, we can get maximum power output as well as the important chemical, hydroxylamine.

The current in Fig. 7 reaches a plateau at cathode potentials of −0.13 to −0.29 V *vs.* Ag/AgCl (corresponding to the terminal voltages of −0.07 to −0.20 V). The application of further negative potential to the cathode (< −0.32 *vs.* Ag/AgCl) enhanced the current again as can be seen in Fig. 7. Under these conditions, hydrogen was pumped from the anode to the cathode which was confirmed by analyzing the gas evolved into the cathode compartment. The enhanced current was ascribed exclusively to this hydrogen pumping.

Active site and reaction mechanism.—Oxidation state of iron in Fe-Pc.—The standard redox potentials of the iron of Fe-Pc were reported to be 0.65 and −0.07 V *vs.* Ag/AgCl for Fe^{3+}/Fe^{2+} and Fe^{2+}/Fe^{+}, respectively.[11] The results in Fig. 6 and 7 indicate that the reduction of NO into hydroxylamine was initiated at a cathode potential more negative than 0.08 V *vs.* Ag/AgCl. The formation of hydroxylamine and the current were accelerated on decreasing the cathode potential from 0.08 to −0.13 V *vs.* Ag/AgCl. These results and the redox potentials of the iron described above suggest that the oxidation state of iron in Fe-Pc working as the active site for the reduction of NO into hydroxylamine must be Fe^{2+}. Easy coordination of NO to Fe^{2+}-Pc has been reported by Collamati *et al.*[12] and Tamaru *et al.*[13] The results in Fig. 6 and 7 showed that the formation of hydroxylamine and the current reached plateaus at a range of −0.13 to −0.29 V *vs.* Ag/AgCl. Under these reaction conditions, the diffusion of NO to the Fe^{2+} site or that of the formed NH_2OH into the electrolyte (aqueous H_2SO_4) may control the formation rate of hydroxylamine. Details, however, are not known at this moment.

Ammonia and N_2O formations.—The results in Table I show that the amounts of ammonia and N_2O obtained over the Fe-Pc/Gr are same as those obtained for the graphite without additives within experimental errors. The results in Fig. 3 indicate that only the formation of hydroxylamine is improved with increasing the content of Fe-Pc in graphite. The formation of ammonia and N_2O did not depend on the addition of Fe-Pc. These observations strongly suggest that the formations of ammonia and N_2O occur on the graphite and that of hydroxylamine specifically on Fe-Pc.

The unique electrocatalytic activity of Fe-Pc for specific formation of hydroxylamine has also been demonstrated in Table II. The formations of N_2O and ammonia observed in Table II are ascribed to the electrocatalytic reactions over the carbon materials used as supporters of Fe-Pc.

Tentative mechanism for the specific catalysis.—It is generally believed that for the electrochemical reduction of nitric oxide to occur, nitric oxide and the first reduction intermediate NHO must adsorb on the active site, here on Fe^{2+} site of Fe-Pc. Further reduction of NHO to NH_2O and NH_2OH on the iron site followed by extraction with H_2SO_4, producing hydroxylamine in an aqueous solution of H_2SO_4. This reaction sequence is demonstrated in Fig. 8.

Over noble metal electrocatalysts such as Pt, Ru, and Pd, the adsorbed NHO may dimerize followed by intramolecular elimination of H_2O, forming N_2O. Moreover, NH_2O or NH_2OH can be reduced further to NH_3. [8] These are what we observed for the noble metals in Table I. However, over Fe-Pc in this work, the observation of the specific formation of hydroxylamine suggests that these reactions do not occur. Although detailed mechanism should be clarified by further studies, we suggest that the dimerization of NHO could be prohibited because the iron sites for adsorption of NHO are isolated from each other by phthalocyanine rings. For reduction of NH_2O and NH_2OH into NH_3, the breaking of the N–O bond is needed. This process must also require more than two adjacent sites. Thus, we believe that the isolation of the iron sites by the phthalocyanine rings is the characteristic that leads to catalytic formation of hydroxylamine.

The results obtained for the $FeSO_4$/Gr cathode in Table I support the discussion described above. It is reasonable to assume that the reduction of NO under short-circuit conditions occurs on Fe^{2+} sites because the standard redox potential of Fe^{3+}/Fe^{2+} is *ca.* 0.57 V *vs.* Ag/AgCl.[14] Compared with the Fe^{2+} sites of Fe-Pc, those in the $FeSO_4$/Gr are not necessarily far isolated each other but may be present nearby which enables the dimerization of NHO and the breaking of N–OH bond. In fact, the $FeSO_4$/Gr cathode in Table I catalyzed the formation of N_2O and NH_3 preferentially to that of hydroxylamine.

In contrast to the electrocatalytic activities of Fe-Pc and $FeSO_4$, iron tetraphenyl porphrin (Fe-TPP) did not show any catalytic activity for NO reduction. The products observed for the Fe-TPP/Gr in Table I were solely due to the reaction on the host graphite. Barley *et al.*[15] suggested a large negative potential (<−0.6 V *vs.* Ag/AgCl) for reduction of NO to NO^- of the nitrosyl complex of iron porphrins. Thus, the electrochemical reduction of NO_2^- through nitrosyl complex to N_2O, NH_2OH, and NH_3 over iron porphrins usually requires a negative potential lower than −0.6 V *vs.* Ag/AgCl.[15] Therefore, under short-circuit conditions in this work (cathode potential *ca.* −0.13 V *vs.* Ag/AgCl), we cannot expect the reduction of NO on the Fe-TPP/Gr cathode.

Acknowledgments

The present work was supported by a Grant-in-Aid for Scientific Research on Priority Areas "Catalytic Chemistry of Unique Reaction Fields" from The Ministry of Education, Science and Culture.

Manuscript submitted Oct. 16, 1995; revised manuscript received May 10, 1996.

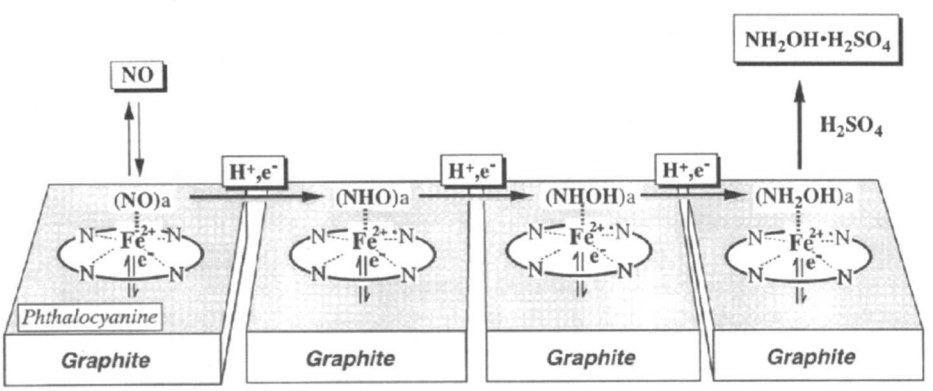

Fig. 8. Reaction sequence of electrochemical reductions of nitric oxide.

Tokyo Institute of Technology assisted in meeting the publication costs of this article.

REFERENCES

1. S. H. Langer and H. P. Landi, *J. Am. Chem. Soc.*, **86**, 4694 (1964).
2. S. H. Langer and S. Yurchak, *This Journal*, **116**, 1128 (1969).
3. R. W. Spillman, R. M. Spotnits, and J. T. Lundquist, Jr., *Chemtech*, 176 (March 1984).
4. C. G. Vayenas, S. I. Bebelis, and C. C. Kyriazis, *Chemtech*, 422 (July 1991).
5. B. G. Snider and D. C. Johnson, *Anal. Chim. Acta*, **105**, 9 (1979).
6. L. J. J. Janssen, M. M. J. Pieterse, and E. Barendrecht, *Electrochim. Acta*, **22**, 27 (1977).
7. M. L. Bathia and A. P. Watkinson, *Can. J. Chem. Eng.*, **57**, 631 (1979).
8. S. H. Langer and K. T. Pate, *Ind. Eng. Chem. Process Des. Dev.*, **22**, 264 (1983).
9. R. L. Pesselman, M. J. Foral, and S. H. Langer, *Anal. Chem.*, **59**, 1239 (1987).
10. *Textbook of Quantitative Inorganic Analysis*, 4th ed., J. Bassett, R. C. Denney, G. H. Jeffery, and J. Mendham, Editors, p. 730, Longman, London (1978).
11. J. Zaga, M. Fáez, A. A. Tanaka, J. R. dos Satos, Jr., and C. A. Linkous, *J. Electroanal. Chem.*, **339**, 13 (1992).
12. I. Collamati, C. Ercolani, and G. Rossi, *Inorg. Nucl. Chem. Lett.*, **12**, 799 (1976).
13. K. Uchida, M. Soma, T. Onishi, and K. Tamaru, *J. Chem. Soc., Faraday Trans. 1*, **75**, 2839 (1979).
14. *Lange's Handbook of Chemistry*, J. A. Dean, Editor, McGraw-Hill, New York (1985).
15. M. H. Barly, K. J. Takeuchi, and T. J. Meyer, *J. Am. Chem. Soc.*, **108**, 5876 (1986).

Critical Analysis of Potentiostatic Step Data for Oxygen Transport in Electronically Conducting Perovskites

Svein Sunde[a]

SINTEF Materials Technology, N-7034 Trondheim, Norway

Kemal Nişancioğlu*

Department of Electrochemistry, Norwegian University of Science and Technology, N-7034 Trondheim, Norway

Turgut M. Gür*

Center for Materials Research, Stanford University, Stanford, California 94305-4045, USA

ABSTRACT

The solid-state potentiostatic technique is a convenient and versatile tool for studying oxygen transport in electronically conducting perovskites. Furthermore, a systematic analysis of the relaxation data helps elucidate the mechanistic nature of the prevalent oxygen rate process. As a case in point, we describe potential step measurements on 90% dense samples of $SrCo_{1-x}Fe_xO_{3-\delta}$, focusing *per se* on the assumptions underlying the technique and the interpretation of results. Careful analysis of the current-relaxation data pointed to the presence of high-diffusivity paths in the samples. It also indicated that the overall transport rate is controlled by an oxygen exchange reaction at the grain boundaries. This complication prevented unambiguous assessment of the chemical diffusion coefficient in this material. In addition, the analysis showed that wide disagreements in the oxygen chemical diffusion coefficients reported in the literature for doped perovskites may be attributed to differences in the sample quality (*e.g.*, density, grain size, and distribution) and the measurement technique employed.

Introduction

The solid-state electrochemical technique and cell design proposed by Belzner *et al.*[1] based on the fundamental framework reviewed by Wen *et al.*[2] is regarded as a convenient method for the assessment of the chemical diffusion coefficient of oxygen in electronically conducting perovskites, because a large amount of data as a function of temperature and oxygen activity can be obtained in a relatively short period from a single specimen.[3] Since the diffusion test additionally yields coulometric titration data,[4] the corresponding ionic conductivity of oxygen can also be calculated. The interpretation of data, however, is usually based on a number of assumptions, of which the most important ones are the absence of rate limitations due to interfacial exchange reactions and one-dimensional diffusion.[2]

An unresolved problem related to oxygen diffusion in perovskites is the existence of large discrepancies in the literature data for similar types of materials obtained by use of various relaxation and tracer techniques, giving, respectively, chemical and tracer diffusion coefficients.[5-8] Conversion of one type of data to another in the conventional manner, even if the data are associated with very large enhancement factors, cannot always explain these large differences. For example, by using the potential-step technique on dense samples, Gür *et al.*[9] found the chemical diffusion coefficient, D, of $La_{0.5}Sr_{0.5}MnO_\xi$ to be of the order 10^{-7} cm^2/s at 830°C and a partial pressure of oxygen $p_{O_2} \simeq 0.21$ atm. Here, $\xi = 3 \pm \delta$, where δ represents the small deviation from the stoichiometric value $\xi = 3$. By correcting for the enhancement factors, a tracer diffusion coefficient, D^*, of the order 10^{-11} cm^2/s was calculated. However, by direct measurement of ^{18}O profiles by secondary ion mass spectroscopy (SIMS), Carter *et al.*[10] found D^* for $La_{0.5}Sr_{0.5}MnO_\xi$ to be about 10^{-14} cm^2/s at 800°C and $p_{O_2} \simeq 0.7$ atm. These discrepancies cannot be explained in terms of small differences in temperature and partial pressure of oxygen if the oxygen is transported by vacancy diffusion.[11,12]

Furthermore, comparisons of results for the same type of diffusion measurements indicate large disagreements. Based on gravimetric relaxation studies, Kjær *et al.*[13] calculated a chemical diffusion coefficient of roughly 10^{-13} cm^2/s for powder samples of $La_{0.8}Sr_{0.2}MnO_\xi$ at 800°C, whereas Gür *et al.*[9] found by use of the potential-step technique, D

* Electrochemical Society Active Member.
[a] Present address: Risø National Laboratory, Materials Department, DK-4000 Roskilde, Denmark.